EPJ Web of Conferences **66**, 03004 (2014)
DOI: 10.1051/epjconf/ 20146603004


# Collective features of nuclear dynamics with exotic nuclei within microscopic transport models

Virgil Baran[1,a], Maria Colonna[2], Massimo Di Toro[2,3], Andreea Croitoru[1], and Daniel Dumitru[1]

[1] *Faculty of Physics, University of Bucharest, Romania*
[2] *Laboratori Nazionali del Sud, INFN, I-95123 Catania, Italy*
[3] *Physics and Astronomy Department, University of Catania, Italy*

**Abstract.** We employ a transport model based on Landau-Vlasov equation to explore the dipolar response of neutron rich systems and its dependence on the symmetry energy. We present evidences for collective features of the Pygmy Dipole Resonance (PDR) and study its dependence with the mass number. We extract a parametrization for the energy centroid position, $41A^{-1/3}$, which agrees quite well with the data for Ni, Zr, Sn and Pb. A linear correlation between the Energy Weighted Sum Rule (EWSR) associated to PDR and the neutron skin thickness is evidenced. An increase of $15 MeV fm^2$ of EWSR to a change of $0.1 fm$ of neutron skin size is obtained. We conclude that different nuclei having close neutron skin size will exhaust the same EWSR in the pygmy region. Consequently a precise experimental estimate of total EWSR exhausted by PDR allows the determination of the neutron skin size and to constrain the slope parameter of the symmetry energy.

## 1 Introduction

The fragmentation facilities at GANIL, GSI, MSU and RIKEN provide important results regarding the behavior of exotic nuclei and stimulated new studies of the nuclear properties over an extended range of the neutrons to protons ratio, N/Z. The emergence of possible new exotic modes of excitation [1] as well as the evolution of the collective features with the number of neutrons in excess are among the most challenging topics in today nuclear physics. In this context an important role is played by the nuclear symmetry energy $E_{sym}$ which determines the effects associated with the difference between the number of neutrons and the number of protons, factorizing the isospin parameter $I = \frac{N-Z}{A}$ in the expression of the total energy per particle of a system at nucleonic density $\rho$, $\frac{E}{A}(\rho, I) = \frac{E}{A}(\rho) + \frac{E_{sym}}{A}(\rho)I^2$. For example, it controls the development of the neutron skin which is expected to influence the properties of collective modes in nuclei far from stability [2–4]. Therefore one of the major tasks of recent investigations is to determine a consistent density parametrization of the symmetry energy in order to obtain a unified picture of nuclear properties below saturation as well as at large compression of asymmetric nuclear matter [5–7]. Indeed, several experiments performed during the last ten years indicate a resonance-like peak in the electric dipole (E1) response well below the GDR, more clear

[a] e-mail: baran@nipne.ro

evidenced in neutron rich nuclei [8–12], see [13, 14] for recent overviews. It exhausts few percentages of dipolar Energy Weighted Sum Rule (EWSR) and its controversial nature attracted a considerable interest for theory too [15].

The important question if a strong correlation between the neutron skin and the low-energy E1 strength can be distinguished was raised by Piekarewicz [16]. Within a relativistic random-phase approximation (RPA) he observed that for Sn isotopes the fraction of EWSR acquired in the energy region between $5MeV$ and $10MeV$ manifests a linear dependence with the neutron skin size up to mass A=120 followed by a mild anti-correlation. However, such a strong correlation was questioned by Reinhard and Nazarewicz [17]. They introduced an investigation based on a covariance analysis aimed to identify a set of good indicators that correlate very well with the isovector properties and suggested that the low-energy E1 strength is very weakly correlated with the neutron skin while the dipolar polarizability should be a much stronger indicator of isovector properties.

Here we shall address the problem of collectivity of PDR and its relation with the neutron skin by adopting an investigation based on a microscopic semi-classical transport model. While the model is unable to account for effects associated with the shell structure, the self-consistent approach based on Landau-Vlasov equations is suitable to describe robust quantum modes, of zero-sound type, in both nuclear matter and finite nuclei allowing for a systematic study over an extended mass and isospin domain. Our aim is to explore if a such description is able to predict a dipolar response different from GDR and to extract basic properties of the new collective mode as the energy centroid position and the acquired EWSR.

## 2 The transport model

We study the collective dynamics of neutron rich nuclei in a model based on the two coupled Landau-Vlasov kinetic equations for neutrons and protons:

$$\frac{\partial f_q}{\partial t} + \frac{\mathbf{p}}{m}\frac{\partial f_q}{\partial \mathbf{r}} - \frac{\partial U_q}{\partial \mathbf{r}}\frac{\partial f_q}{\partial \mathbf{p}} = I_{coll}[f_n, f_p], \tag{1}$$

which determine the evolution of the one-body distribution functions $f_q(\vec{r}, \vec{p}, t)$, with $q = n, p$ [5]. Since we shall focus mainly on the dynamics of various collective modes and not on their collisional damping in the following we do not consider the collision integral. We have tested however that the results are not strongly influenced, as expected, when it is included. From the one-body distribution functions one obtains the local densities $\rho_q(\vec{r}, t) = \int \frac{2d^3\mathbf{p}}{(2\pi\hbar)^3} f_q(\vec{r}, \vec{p}, t)$ and define the isoscalar density $\rho_{isoscalar} = \rho = \rho_n + \rho_p$ and the isospin or isovector density $\rho_{isovector} = \rho_i = \rho_n - \rho_p$. The nuclear mean-fields $U_q$ appearing in Eq. (1) are derived within an Energy Density Functional (EDF) approach where the total energy of the system $E = \int d^3r\,(\mathcal{E}_{kin}(\mathbf{r}) + \mathcal{E}_{pot}(\mathbf{r}))$ is obtained starting from an effective interaction of Skyrme-like ($SKM^*$) type [18]. The interaction contribution to the energy density is:

$$\mathcal{E}_{pot}(\rho, \rho_i) = \frac{A}{2}\frac{\rho^2}{\rho_0} + \frac{B}{\sigma+1}\frac{\rho^{\sigma+1}}{\rho_0^{\sigma}} + \frac{C(\rho)}{2}\frac{\rho_i^2}{\rho_0} \quad , \tag{2}$$

The functional derivative of $\mathcal{E}_{pot}$ with respect to the proton (neutron) density $U_q(\rho) = \delta\mathcal{E}_{pot}(\mathbf{r})/\delta\rho_q(\mathbf{r})$ leads to:

$$U_p = A\frac{\rho}{\rho_0} + B\Big(\frac{\rho}{\rho_0}\Big)^{\sigma} - C(\rho)\frac{\rho_i}{\rho_0} + \frac{1}{2}\frac{dC(\rho)}{d\rho}\frac{\rho_i^2}{\rho_0} \quad , \tag{3}$$

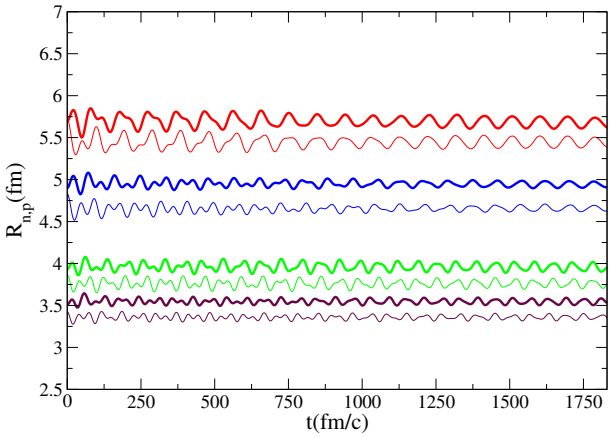


**Figure 1.** The time evolution of the neutron mean square radius $R_n$ (thick lines) and of the proton mean square radius $R_p$ (thin lines) after a weak perturbation of the ground state. From the top the pairs of lines correspond to $^{208}Pb$ (red), $^{132}Sn$ (blue), $^{68}Ni$ (green) and $^{48}Ca$ (maroon). The asystiff EOS case.

$$U_n = A\frac{\rho}{\rho_0} + B\Big(\frac{\rho}{\rho_0}\Big)^{\sigma} + C(\rho)\frac{\rho_i}{\rho_0} + \frac{1}{2}\frac{dC(\rho)}{d\rho}\frac{\rho_i^2}{\rho_0} \quad . \tag{4}$$

In the spirit of EDF formalism the coefficients $A, B$ and $\sigma$ are chosen in order to reproduce the saturation properties of symmetric nuclear matter with $\rho_0 = 0.16fm^{-3}$, $E/A = -16MeV$ and a compressibility modulus $K = 200MeV$. The resulting values are $A = -356MeV$, $B = 303MeV$, $\sigma = 7/6$. Even if the energy functional is obtained from an effective interaction and a many-body variational method, there are several subtle differences between HF and EDF approach since the coefficients factorizing terms which are functions of the local density (and possibly more general of the density gradients) are adjusted by requiring that a set of experimental properties such as the saturation density, the binding energy at saturation, the compressibility modulus, the symmetry energy at saturation and possibly other features are reproduced. Therefore, these coefficients encode more physics than those provided within HF theory. In the isovector sector, based on the philosophy of EDF, while keeping the value of symmetry energy at saturation almost the same, we shall allow for three different dependences with density away from equilibrium. For the asysoft EOS we imply a Skyrme-like, SKM*, parametrisation with $\frac{C(\rho)}{\rho_0} = (482 - 1638\rho)MeVfm^3$ which leads to a slope parameter $L = 3\rho_0\frac{dE_{sym}/A}{d\rho}|_{\rho=\rho_0}$ small $L = 14.4MeV$. For the asystiff EOS the coefficient $C(\rho)$ is constant (i.e $C(\rho) = constant \approx 32MeV$), the slope parameter being $L = 72.6MeV$. Lastly, for the asysuperstiff EOS, $\frac{C(\rho)}{\rho_0} = \frac{32}{\rho_0}\frac{2\rho}{(\rho+\rho_0)}$, the symmetry term increases rapidly around saturation density being characterized by a value of slope parameter $L = 96.6MeV$.

The integration of the transport equations is based on the test-particle (t.p.) method [19], with a number of 1300 t.p. per nucleon in the case of Sn isotopes, ensuring in this way a good spanning of the phase-space.

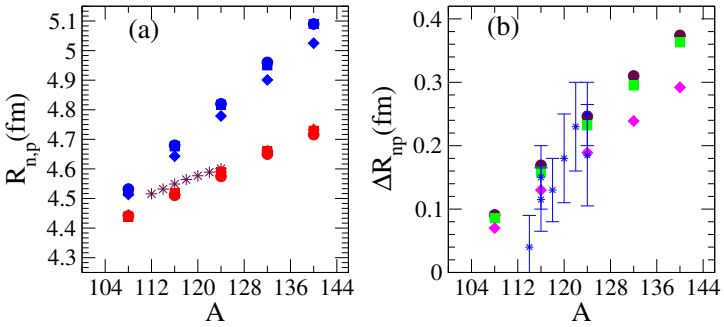


**Figure 2.** (a) The neutron (blue) and proton (red) mean-square radius for Sn isotopes: asysoft (diamonds), asystiff (squares) and asysuperstiff (circles) EOS. The stars are experimental data from Refs. [20]. (b) The neutron skin size as a function of mass for Sn isotopes: asysoft (magenta diamonds) asystiff (green squares), asysuperstiff (maroon circles). The stars and the error bars (blue) are experimental data from Ref .[21].

## 3 Results and discussion

Since we intend to investigate the possible correlations between the neutron skin and the properties of PDR we explore first the prediction of the model for the mean-square radius of proton and neutron distributions. The width of the neutron skin is defined as $\Delta R_{np} = \sqrt{\langle r_n^2 \rangle} - \sqrt{\langle r_p^2 \rangle} = R_n - R_p$ where $\langle r_q^2 \rangle = \frac{1}{N_q} \int r^2 \rho_q(\vec{r}, t) d^3\mathbf{r}$. The symmetry energy dependence of $\Delta R_{np}$ is studied by considering in the mean-field structure the parametrizations with the density of the coefficient $C(\rho)$ mentioned in the previous section. We shall analyze the systems $^{48}$Ca, $^{68}Ni$, $^{86}Kr$ and $^{208}Pb$, as well as a chain of Sn isotopes, $^{108,116,124,132,140}Sn$. A direct method to obtain the values of $R_n$ and $R_p$ is by observing their small oscillations around equilibrium values after a gentle perturbation, see the Fig. 1.

We remark that the numerical simulations keep a very good stability of the dynamics for at least $1800 fm/c$. Using this procedure we obtain for the charge mean square radius of $^{208}Pb$ a value around $R_p = 5.45 fm$, quite close to the experimental value $R_{p,exp} = 5.50 fm$. For Sn isotopes we display the mass dependence of $R_n, R_p$ in Fig. 2 (a) and of $\Delta R_{np}$ respectively in Fig. 2 (b).

For the charge radii the predictions from the three asy-EOS virtually coincide and we observe a good agreement with the experimental data reported in [20]. For all adopted parametrizations the predicted values of the neutron skin thickness are within the experimental errors bars, see the data presented in [21] for the stable Sn nuclei. In the case of $^{208}Pb$ we find $\Delta R_{np} = 0.19 fm$ for asysoft, $\Delta R_{np} = 0.25 fm$ for asystiff and $\Delta R_{np} = 0.27 fm$ for asysuperstiff EOS while for $^{68}Ni$ the corresponding values are $\Delta R_{np} = 0.17, 0.19, 0.20 fm$. We see that the neutron skin thickness increases with the slope parameter L, an effect related to the tendency of the system to stay more isospin symmetric even at lower densities when the symmetry energy changes slowly below saturation, as is the case for asy-soft EOS.

We study the E1 response considering a GDR-like initial condition [22], which is associated to the instantaneous excitation $V_{ext} = \eta \delta(t - t_0)\hat{D}$ at $t = t_0$ [23]. In this case, a boost of all neutrons against all protons is induced while keeping the Center of Mass (CM) at rest. Here $\hat{D}$ is the dipole operator. If $|\Phi_0\rangle$ is the state before perturbation then the excited state becomes $|\Phi(t_0)\rangle = e^{i\eta\hat{D}}|\Phi_0\rangle$. The value of $\eta$ can be related to the initial expectation value of the collective dipole momentum $\hat{\Pi}$,

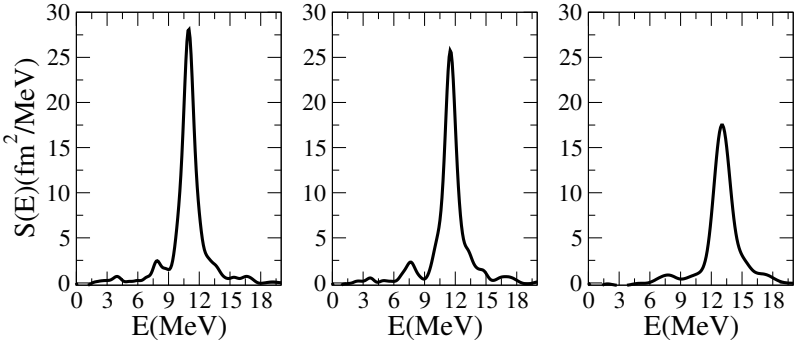


**Figure 3.** The strength function for $^{132}Sn$: asysuperstiff (left), asystiff (center) and asysoft (right) EOS.

$\langle\Phi(t_0)|\hat{\Pi}|\Phi(t_0)\rangle = \hbar\eta\frac{NZ}{A}$. Here $\hat{\Pi}$ is canonically conjugated to the collective coordinate $\hat{X}$ which defines the distance between the CM of protons and the CM of neutrons, i.e. $[\hat{X},\hat{\Pi}] = i\hbar$ [24].

Then the strength function $S(E) = \sum_{n>0}|\langle n|\hat{D}|0\rangle|^2\delta(E-(E_n-E_0))$, directly related to the excitation probability in unit time, where $E_n$ are the excitation energies of the states $|n\rangle$ while $E_0$ is the energy of the ground state $|0\rangle = |\Phi_0\rangle$, is obtained from the imaginary part of the Fourier transform of the time-dependent expectation value of the dipole momentum $D(t) = \frac{NZ}{A}X(t) = \langle\Phi(t)|\hat{D}|\Phi(t)\rangle$ as

$$S(E) = \frac{Im(D(\omega))}{\pi\eta\hbar} = \frac{A}{NZ}\frac{Im(D(\omega))}{\pi\langle\Phi(t_0)|\hat{\Pi}|\Phi(t_0)\rangle}, \tag{5}$$

where $D(\omega) = \int_{t_0}^{t_{max}} D(t)e^{i\omega t}dt$. We follow the dynamics of the system until $t_{max} = 1830fm/c$ for an initial perturbation along the z-axis. At $t = t_0 = 30fm/c$ we determine the collective momentum which appears in Eq. (5). A filtering procedure, as described in [25], was applied in order to eliminate the artifacts resulting from a finite time domain analysis of the signal. A smooth cut-off function was introduced such that $D(t) \to D(t)cos^2(\frac{\pi t}{2t_{max}})$. For the three asy-EOS the E1 strength functions of $^{132}Sn$ are represented in Fig. 3. We compared the numerically estimated value of the first moment $m_1 = \int_0^\infty ES(E)dE$ with that expected from the Thomas-Reiche-Kuhn (TRK) sum rule $m_1 = \frac{\hbar^2}{2m}\frac{NZ}{A}$ and concluded that the differences were of only few percentages. The observed difference is a measure of the accuracy of our procedure to extract the dipolar collective response of neutron rich systems.

We applied this method to the systems mentioned above. In all cases a well defined peak situated at energies below GDR energy,which we associate with Pygmy Dipole Resonance, was identified. The energy centroid of PDR for $^{208}Pb$ is located around $7.0MeV$ in good agreement with recent experimental data which indicate $E_{PDR,Pb} = 7.36MeV$ [11]. For $^{68}Ni$ we obtain $9.8MeV$, very close to the recent reported data $E_{PDR,Ni} = 9.9MeV$ [26]. We observe that GDR energy centroid is underestimated in comparison with the experimental results, a fact related with the choice of the interaction which has not an effective mass [27]. A clear dependence with the slope parameter manifests as a consequence of the isovector nature of the mode. This feature shows that also the symmetry energy values below saturation are affecting the dipole oscillations of the finite systems. The Fig. 4 displays the position of the PDR energy centroid as a function of mass for all studied systems (blue circles). In addition, we represent the position of the PDR energy peaks as results from the power spectrum analysis of the pygmy dipole $D_y(t)$ after a pygmy-like initial condition, see [22] (red diamonds) and the experimental

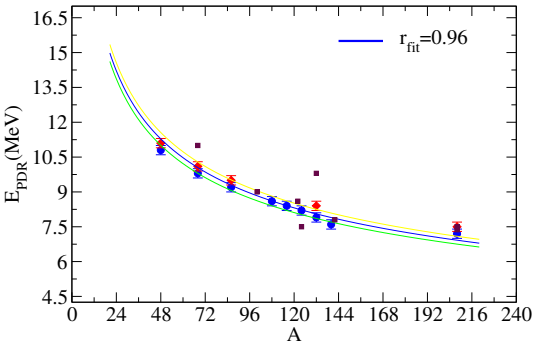


**Figure 4.** The energy centroid of PDR as a function of mass (blue circles and red diamonds). The solid lines correspond to parametrizations $40A^{-1/3}$ (green), $41A^{-1/3}$ (blue) and $42A^{-1/3}$ (yellow). The maroon squares are experimental data from Ref. [28]. $r_{fit}$ refers to the correlation coefficient.

data available from the works where information about the position of the low-energy E1 centroid was reported (maroon square) [28]. The differences between the two methods are within a half of MeV. An appropriate parametrization, obtained from the fit of numerical results is $E_{PDR} = 41A^{-1/3}$. This parametrization corresponds to the distance between major shells and is close to what is expected in the harmonic oscillator shell model (HOSM) approach [24]. We notice the agreement with several recent experimental data. While the isovector residual interaction pushes up the value of the GDR energy it seems that the PDR energy centroid is not much affected by this part of the interaction. This feature may explain the better agreement with experimental observations in comparison with the GDR case.

Having obtained the strength function we can calculate the nuclear dipole polarizability $\alpha_D = 2e^2 \int_0^\infty \frac{S(E)}{E} dE$ as an additional test of our method. In the case of $^{68}Ni$ $\alpha_D$ it changes from $4.1 fm^3$ and $5.7 fm^3$ when we pass from asysoft to asysuperstiff EOS while for $^{208}Pb$ it varies from $21.1 fm^3$ to $28.6 fm^3$, in a resonable agreement with experimental measurements.

By integration over the resonance region associated with PDR we can obtain the EWSR exhausted by the this mode:

$$m_{1,y} = \int_{PDR} ES(E)dE \tag{6}$$

The dependence of the moment $m_{1,y}$ on the neutron skin thickness is shown in Fig. 5, where the informations concerning all mentioned systems for the three asy-EOS were included. While below $0.15 fm$ the EWSR acquired by PDR manifests a saturation tendency, above this value a linear correlation clearly manifests. For the same system, when we pass from asysuperstiff to asysoft parametrisation, the neutron-skin shrinks and correspondingly the value of $m_{1,y}$ decreases. This behavior is in agreement with the results reported in [33] in a self-consistent RPA approximation based on a relativistic energy density functionals. Moreover we notice that the variation rate appears to be system independent, obtaining an increase of $15 MeV fm^2$ of the exhausted EWSR to a change of $0.1 fm$ of the neutron skin width. Such features suggest that the acquired EWSR should not differ too much even for different nuclei if they have close values of the neutrons skin thickness.

We would like to mention that these findings look qualitatively in agreement with those of Inakura [34], based on systematic calculations within a RPA with Skyrme functional SkM* treatment, where a

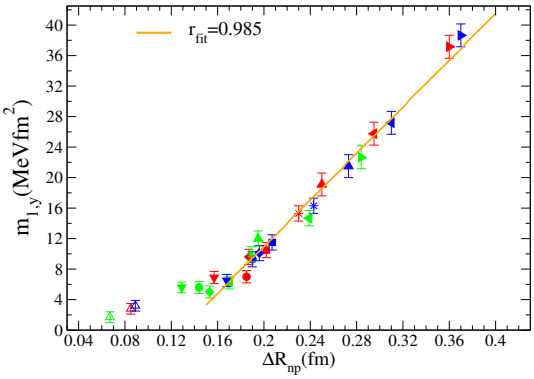


**Figure 5.** The EWSR exhausted by PDR as a function of neutron skin in $^{108}Sn$ (empty triangles up), $^{116}Sn$ (triangles down), $^{124}Sn$ (stars), $^{132}Sn$ (triangles left), $^{140}Sn$ (triangles right, $^{48}Ca$ (circles), $^{68}Ni$ (squares), $^{86}Kr$ (diamonds), $^{208}Pb$ (full triangles up) for asysoft (green), asystiff (red) and asysuperstiff (blue) EOS. $r_{fit}$ refers to the correlation coefficient. The error bars are related to the uncertainties in defining the integration domain for the PDR response.

linear correlation of the fraction of EWSR exhausted in the low-energy region was evidenced for several isotopic chains. These results may also suggest a possible new sum-rule type relation connecting the neutron skin thickness to the EWSR exhausted by PDR.

Summarizing, we addressed some open questions raised recently [14] regarding the nature of PDR within a microscopic semi-classical transport approach which is based on Landau-Vlasov equations. A systematic analysis was performed evidencing a low-energy dipole collective mode in all studied systems. We extracted a dependence of the PRD energy centroid with mass very well described by the parametrization $E_{PDR} = 41A^{-1/3}$, in agreement with several recent experimental informations. This mass dependence suggests a close connection with the characteristic frequency of the HOSM, $\hbar\omega_0 = 41A^{-1/3}$, as well as a weak influence of the residual interaction in the isovector sector. Such behavior can be related to the isoscalar-like nature of this mode. From our calculations an universal, linear correlation of the EWSR exhausted by PDR with the neutron skin thickness occurs. It appears as a very specific signature, showing that the neutrons which belong to the skin play an essential role in shaping the E1 response in the PDR region. However this fact should not lead to an oversimplified picture of PDR as corresponding to the oscillations of excess neutrons against the inert isospin symmetric core. Within the same transport model the dynamical simulations show a more complex structure [22] which includes an isovector excitation of the core also for the pygmy-like oscillations. These new findings can be useful for systematic experiments searching for this, quite elusive, mode. A precise estimate of EWSR acquired by PDR will provide indications about the neutron skin size which in turn will add more constraints on the slope parameter $L$ of the symmetry energy.

## 4 Acknowledgements

This work for V. Baran and A. Croitoru was supported by a grant of the Romanian National Authority for Scientific Research, CNCS - UEFISCDI, project number PN-II-ID-PCE-2011-3-0972.

## References


[1] N. Paar, D. Vretenar, E. Khan, G. Colo, Rep. Prog. Phys. **70**, 691 (2007).
[2] P. Van Isacker, M.A. Nagarajan, D.D. Warner, Phys. Rev. **C 45**, R13 (1992).
[3] A. Carbone et al., Phys. Rev. **C 81**, 041301(R) (2010).
[4] O. Wieland, A. Bracco, Prog. Part. Nucl. Phys. **66**, 374 (2011).
[5] V.Baran, M. Colonna, M. Di Toro, V. Greco, Phys. Rep. **410**, 335 (2005).
[6] Li Bao-An, Lie-Wen Chen, Che Ming Ko, Phys. Rep. **464**, 113 (2008).
[7] M. Di Toro, V.Baran, M. Colonna, V. Greco, J. Phys. G-Nucl. Part. Phys. **37**, 083101 (2010).
[8] P. Adrich et al., Phys. Rev. Lett. **95**, 132501 (2005).
[9] O. Wieland et al., Phys. Rev. Lett. **102**, 092502 (2009).
[10] A. Klimkiewicz et al., Phys. Rev. **C 76**, 051603(R) (2007).
[11] A. Tamii et al., Phys. Rev. Lett. **107**, 062502 (2011).
[12] T. Kondo et al., Phys. Rev. **C 86**, 014316 (2012).
[13] T. Aumann and T. Nakamura, Phys. Scr. **T 152**, 014012 (2013).
[14] D. Savran, T. Aumann and A. Zilges, Prog. Part. Nucl. Phys. **70**, 210 (2013).
[15] N. Paar, J. Phys. G: Nucl. Part. Phys. **37**, 064014 (2010).
[16] J. Piekarewicz, Phys. Rev. **C 73**, 044325 (2006).
[17] P.-G Reinhard and W. Nazarewicz, Phys. Rev. **C 81**, 051303(R) (2010).
[18] M. Colonna, M. Di Toro, A. B. Larionov, Phys. Lett. **B 428** 1 (1998).
[19] C. Gregoire et al.,Nucl. Phys. **A 465**, 77 (1987); D. Idier et al., Nucl. Phys. **A 564**, 204 (1993).
[20] C.W. De Jager et al., At. Data Nucl. Data Table **36**, 495 (1987); G. Audi and A.H. Wapstra, Nucl. Phys. **A 595**, 409 (1995).
[21] A. Krasznahorkay et al., Phys. Rev. Lett. **82**, 3216 (1999).
[22] V. Baran, B. Frecus, M. Colonna, M Di Toro, Phys. Rev. C **85**, 051601 (2012).
[23] F. Calvayrac, P.G. Reinhard, E. Suraud, Ann. Phys. **225**, 125 (1997).
[24] V. Baran et al., Rom. J. Phys. **57**, 36 (2012).
[25] P.-G. Reinhard, P.D. Stevenson, D. Almehed, J.A. Maruhn, M.R. Strayer, Phys. Rev. **E 73**, 036709 (2006).
[26] D. Rossi, INPC2013, Firenze, Italy and private communication; D. Rossi et al., J. Phys. Conf. Ser. 012072 (2013).
[27] E, Suraud, M. Pi, P. Schuck, Nucl. Phys. A **482**, 187c (1988).
[28] For $^{68}Ni$ from [9]; for $^{100}Mo$ from [29];for $^{122}Sn$ from [30]; for $^{124}Sn$ from [31]; for $^{132}Sn$ from [8]; for $^{142}Nd$ from [32]; for $^{208}Pb$ from [11, 12].
[29] G. Rusev et al., Eur. Phys. J. A **27**, 171 (2006).
[30] H.K. Toft et al., Phys. Rev. **C 83**, 044320 (2011).
[31] J. Endres et al., Phys.Rev. Lett. **105**, 212503 (2010).
[32] C.T. Angell et al., Phys. Rev. **C 86**, 051302(R) (2012).
[33] D. Vretenar, Y.F. Niu, N. Paar, J. Meng, Phys. Rev. **C 85**, 044317 (2012).
[34] T. Inakura, T. Nakatsukasa, K. Yabana, Phys. Rev. **C 84**, 021302(R) (2011)